A Thrust Stand for High-power Steady-state Plasma Thrusters

L.D. Cassady,* A.D. Kodys,† and E.Y. Choueiri‡
Electric Propulsion and Plasma Dynamics Laboratory (EPPDyL)
Mechanical and Aerospace Engineering Department
Princeton University, Princeton, New Jersey 08544

(Dated: July 18, 2002)

The operation of an inverted-pendulum thrust stand to measure thrust for high-power steady-state plasma thrusters is presented. An extensive calibration procedure that characterizes the thrust stand response to thrust and forces induced by the interaction of current carrying conductors is discussed. Techniques are also described that reduce thrust measurement errors induced by thermal effects on the stand. Sensitivities of 3.00±0.32 mV/mN are achieved using a laser-based system to measure stand deflection. Data taken with the 30 kW Lorentz Force Accelerator with lithium vapor propellant operating at 500 A, 9.5 mg/s lithium flow rate and a 0.07 T applied field give a measured thrust of 265±48 mN and a nominal 20% thrust efficiency.

I. INTRODUCTION

High-power electric propulsion systems have long been recognized as among the most promising options for heavy-payload orbit raising and piloted planetary missions [1], [2], but they have lagged behind their lower-power counterparts in laboratory testing. With NASA's renewed interest in the development of nuclear power systems for spacecraft, the steady-state spacecraft power necessary for the practical application of these thrusters may soon be available. The difficulties of laboratory experiments with steady-state plasma thrusters at power levels exceeding tens of kilowatts are numerous. Pumping, power, and cooling requirements necessitate large, expensive facilities. Analytical and numerical models can provide some insight, but performance data are required to validate their results and assumptions. Critical to determining performance, the measurement of steady-state thrust has proven to be a unique challenge.

The problem of high-power steady-state thrust measurement for plasma thrusters is not a simple one. The low thrust-to-weight ratio of these devices (≈25 mN/kg) results in poor thrust resolution with standard pendulum designs. Thermal loads due to the conduction of steady-state current and radiation from the thruster influence the behavior of the thrust stand. Finally, electromagnetic forces imparted to the stand through interactions of the thruster current with the applied magnetic field coils and other current conductors must be accurately measured. We have chosen an inverted-pendulum design based upon that of Haag [4]. Details of the theory, implementation, and calibration are presented in this paper. We will show that the design constraints mentioned above make the careful calibration of the thrust stand and the method of data acquisition critical to obtaining accurate thrust measurements.

The inverted-pendulum thrust stand described here is used as an integral part of our lithium Lorentz Force Accelerator (LiLFA) research program. The demonstration of 50% efficiency at 0.5 MW with 500 hours of nearly erosion-free operation [3] have put LiLFAs at the forefront of high-power electric propulsion research. A 30 kW applied-field thruster, designed and manufactured at the Moscow Aviation Institute (MAI), is currently being investigated. The use of alkali-metal propellants introduce additional difficulties in obtaining accurate thrust measurements. Heating is required to vaporize the propellant, adding to the thermal loading of the thrust stand. Also, more complicated feeding systems, in our case a mechanical-piston system located on the thrust stand, must be considered.

Section II focuses on the theory and operation of the inverted-pendulum thrust stand. In section III we present the primary components of the thruster, its subsystems, and the experimental facilities. The challenges of accurate thrust measurement are covered in section IV. A detailed description of the thrust stand calibration and data analysis is given in section V. Finally, sample thrust data taken during a recent firing of the MAI thruster are presented in VI.

II. THRUST STAND

The thrust stand used to measure steady-state thrust is based on the concept of an inverted-pendulum, as will be described in section II A. Obtaining accurate thrust measurements using the inverted-pendulum design depends critically on three factors;

*Graduate Student, National Science and Engineering Graduate Fellow; Electronic address: lcassady@princeton.edu
†Graduate Student, NASA Graduate Student Research Program
‡Chief Scientist EPPDyL, Associate Professor, Applied Physics Group. Associate Fellow, AIAA.

- Maintaining an accurate knowledge of the sensitivity of the stand as it deflects due to thruster operation.
- Maintaining the stand near its vertical position where the deflection is a linear function of the force applied, the stand sensitivity is near its maximum and the thermal drifts are minimized.
- An accurate accounting of forces other than thrust on the stand.

These factors effect every aspect of the thrust stand design and thruster operation, as will be shown in this section. Section II B will describe the design of the thrust stand. The method of thrust measurement is described in section II C.

A. Inverted-Pendulum Thrust Stand Theory

Unlike a standard pendulum, in which it takes a larger force to move a heavier mass through the same deflection angle, an inverted-pendulum takes advantage of the weight of the thruster to amplify the deflection due to the applied force. For small deflections:

$$d = \frac{FL}{g\left[M_\star - M\right]} \tag{1}$$

where d is the horizontal stand displacement, F the total force applied to the stand, L the length of the flexures, M the mass supported by the stand and $M_\star$ is a characteristic mass which depends upon the stand characteristics. $M_\star$ is defined as:

$$M_\star \equiv Lk/g \tag{2}$$

where k the effective spring constant, or elasticity, of the stand flexures.

From equation 1, it is clear that the sensitivity of the stand, defined as the ratio of stand displacement to applied force, will increase as the mass, M, approaches the value of the characteristic mass, $M_\star$. We have not attempted to modify the the stand weight to approach the characteristic mass, but rather we attempt to characterize the sensitivity of the stand under experimental conditions. It is also clear that the stand displacement is directly proportional to the applied force. As will be seen later, we measure the change in the *angle* of the stand tilt, not the stand displacement. Because of the small angles of deflection we can assume a linear relation between force and angle and this was verified by the calibration.

B. Thrust Stand Description

There are two primary components of the thrust stand: 1) the flexures that serve as the pendulum arm and support and 2) the aluminum support structure for the thruster and feed system. A schematic of the thrust stand, whose initial design and implementation is described in [5], is shown in Fig. 1. The pendulum arm consists of nine parallel "b" shaped 3/8" diameter copper tubes. The flexures are held in place at their base by a fiberglass beam attached to the vacuum chamber. Thin (5 mil), 5 cm wide sections of flexural brass sheet attached to either side of the main flexures limit stand twisting. The aluminum support structure is mounted to the top of the flexures by another fiberglass beam.

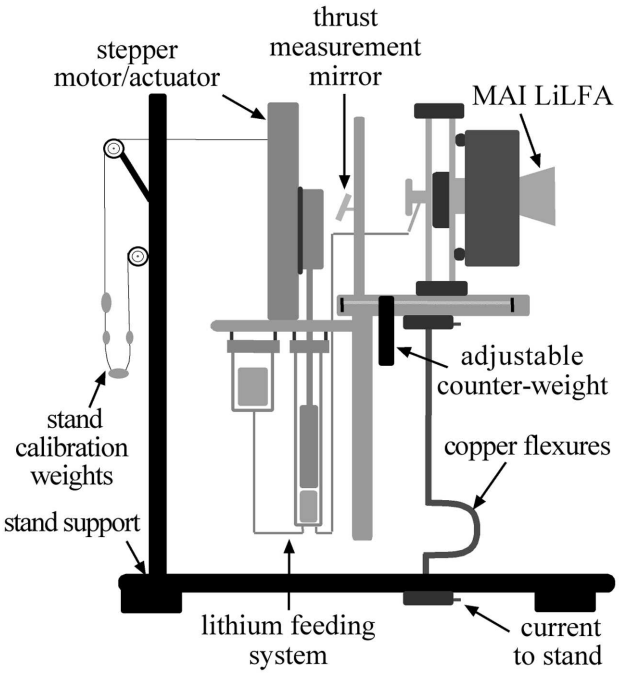

FIG. 1: The schematic of the inverted-pendulum thrust stand, thruster and lithium feed system.

The copper flexures fulfill three important purposes:

- Support and serve as the pivot point of the thrust stand.
- Conduct electrical power for the thruster components and subsystems.
- Carry cooling water to the thruster and subsystems located on the stand.

Electrical power for the thruster, cathode heater, and solenoid is brought to the base of the thrust stand via copper wires. The flexures carry the power to the top of the stand where it is distributed to the thruster and various sub-systems. Cooling water is delivered to the flexures and circulated through the thrust stand components.

A series of four calibration weights attached to the stand via a pulley/motor system allow for *in-situ* calibration of the stand. A total of 534 mN can be added

to the stand immediately prior to and after taking thrust data to ensure a constant sensitivity during the measurement. Normally two weights (267 mN) are added at a time determine the thrust stand sensitivity.

A counterweight system has been developed to correct for large stand drifts due to thermal loading. It is important to maintain the stand near vertical to accurately measure thrust. The tendency of the stand to drift into regions of non-linear and low sensitivity are compensated for by adjusting the center of mass of the stand. Approximately 10 kg of weight can be moved forward or backward relative to the flexures via a remotely controlled motor to re-adjust the center of mass of the stand. A Crossbow CXTA-01-T tilt sensor measures the inclination angle of the stand throughout the experiment to aid in maintaining the stand near its vertical position.

C. Laser-based Deflection Measurement

Using a Linear Voltage Displacement Transducer (LDVT) proved to be impractical for high-power, steady-state thrust measurement. The stand drifts several millimeters during the heat-up of the feed system and cathode, which is not commensurate with the close tolerances required for an LVDT. In addition to drifts in the direction of thrust, a small amount of twisting occurs which makes alignment of an LVDT difficult, if not impossible.

A laser-based optical measurement system has been developed to measure stand deflection and is shown in Fig. 2. Stand deflection is determined by measuring the *angle* through which the stand moves when a force is applied. To increase the sensitivity of the measurements we desire the longest possible laser path length from the stand to the sensor. This is accomplished with a series of mirrors within the chamber. The total path length of the beam is approximately 2 m. The components are:

- A 3 mW Helium-Neon laser mounted on the outside of the vacuum chamber and directed at the thrust stand through a Pyrex window.
- A 5 cm diameter mirror mounted at approximately 45° relative to the laser beam on the stand.
- Three 5 cm diameter mirrors mounted within a box above the thrust stand for protection from lithium.
- The primary component of the system is a 2-D Position Sensing Detector (PSD) manufactured by On-Trak. The 1 cm by 1 cm photodetector array determines the centroid of an incident light source. The output is a two dimensional position ($\pm$5 V) which is independent of the intensity of the incident beam.
- A 52 mm lens with a 2 m focal length positioned just in front of the laser to maintain a focused beam at the detector.

The laser-based thrust measurement system has proven to be immune to many of the problems that plague the LVDT. It is not adversely effected by radio-frequency noise generated by the thruster or thermal drifts of the thrust stand, and most of its components can be placed away from the thruster. It can also be configured to measure different magnitudes of stand deflection simply by changing the path length of the laser beam. Sensitivities of 3.0 mV/mN are easily achievable with this configuration, translating to a 1.5 V signal at nominal thruster operating conditions (500 mN thrust).

III. EXPERIMENTAL APPARATUS

The steady-state low-power facility (SSLPF) at EPPDyL has been designed to measure thrust of alkali metal propellant steady-state LFAs. Presently, the experimental apparatus is equipped to operate with the Moscow Aviation Institute 30 kW LiLFA, described in the next subsection. The lithium feed system that supplies propellant to the thruster is described in the section III B. Section III C describes the facilities and equipment required to support the MAI LiLFA thrust measurement.

A. MAI LiLFA

The 30 kW thruster used in this investigation, Fig.3, was developed and manufactured at the Moscow Aviation Institute under a NASA-JPL contract [6], [7]. Unlike the vapor-fed open-heat-pipe thruster developed by EPPDyL and Thermacore [5], the MAI LiLFA relies on being fed *liquid* lithium that is vaporized inside the cathode. The profiled anode is made of tungsten by plasma spraying and with the profiled surface corresponding to the flux lines of the applied magnetic field. The cathode is a multichannel hollow cathode design. The body is of tungsten and has an outer diameter of 24 mm. Lithium enters the cathode as a liquid and travels through an internal spiral-shaped channel that surrounds a 1.3 kW lithium-vaporizing graphite heater. The front of the cathode is packed with tungsten wire 1.5-2 mm in diameter recessed 6 mm from the exit plane to form the channels. The electrical insulator is aluminum boron nitride. Power to the thruster and cathode heater is supplied to molybdenum flanges. The external, mostly axial, magnetic

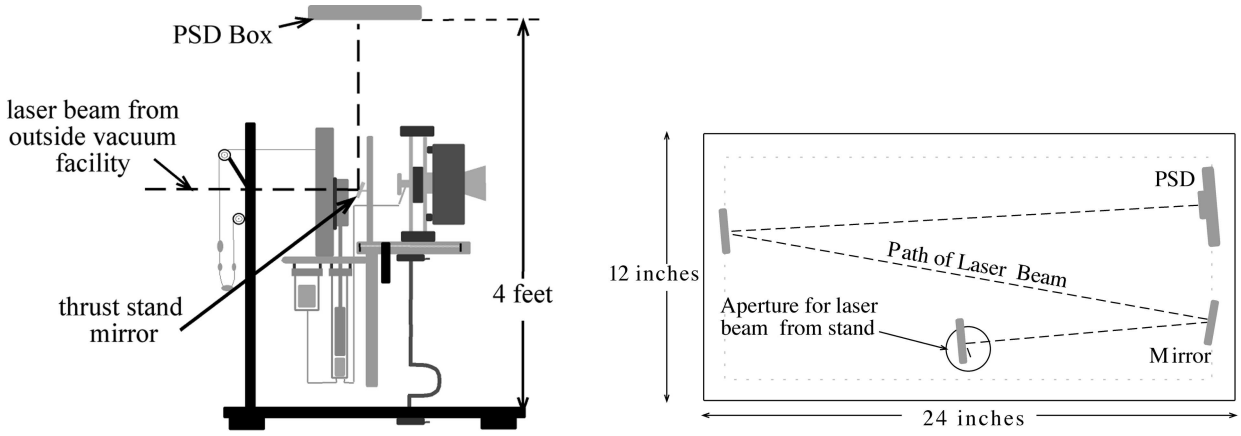

FIG. 2: The layout of the components of the laser-based thrust measurement system.
Left: The position of the mirror on the thrust stand and the box containing the PSD and mirrors.
Right: The top view of the system box.

field is generated by a water-cooled solenoid surrounding the anode. The coil is 56 turns of 8 mm diameter copper tubing, which at 100 A produces a 0.032 T at the cathode tip.

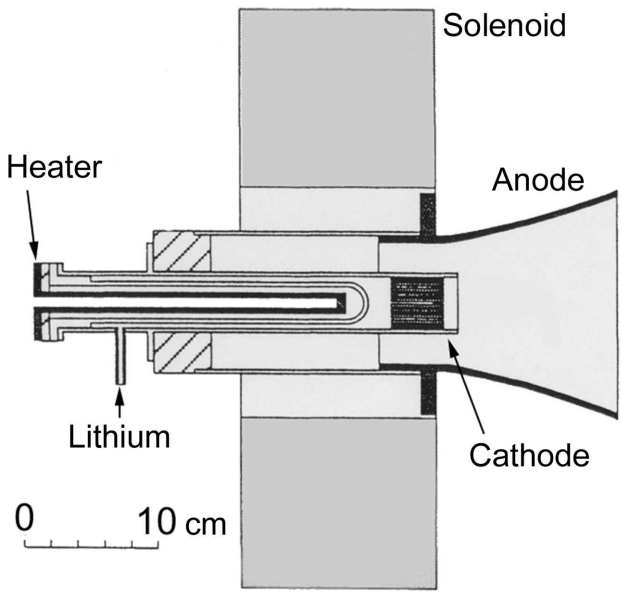

FIG. 3: A schematic of the 30 kW MAI thruster.

With the cathode preheated to approximately 1200° C and no applied magnetic field, reliable thruster ignition occurs with 80 V applied across the electrodes and a nominal lithium flow rate of 9.5 mg/s. Once established, the arc will provide additional cathode heating increasing the vaporization rate of the lithium as it enters the cathode allowing for operation at larger mass flow rates. The stabilization of the vaporization point within the cathode, and therefore the lithium flow rate, is reported in MAI data to occur 6-15 minutes after ignition.

B. Lithium Feed System

A mechanically-driven lithium feeding system was developed through a collaboration between EPPDyL and the Advanced Propulsion Group at JPL, [8]. It supplies liquid lithium to the vaporizer cathode within the MAI thruster. Lithium mass flow is directly proportional to piston speed and is determined by calibration. The calibration resulted in a coefficient of 819 ± 4 mg/mm. Flow rates of 10-120 mg/s are achievable with an error of 1%.

A schematic of the system is shown in Fig. 4 with arrows indicating the path of lithium flow through the system. Solid lithium is loaded into the vacuum facility under argon via the leak-tight reservoir. Under vacuum, the lithium is then melted and fed into the lithium chamber below the piston. Chilled water applied to the feed line between the reservoir and chamber solidifies ($< 180°$ C) the lithium there, forming a plug, and preventing back-flow to the reservoir during thruster operation. A stepper motor and controller set the piston speed and allow for continuous feedback on speed and position as the lithium is fed to the thruster. A chilled-water loop above the lithium chamber "freezes" the lithium there preventing leakage during feeding. Liquid lithium temperatures are maintained between 200 and 300° C during operation.

The entire system is positioned on the thrust stand behind the thruster so as not to impede the free motion of the stand. Alumina insulators electrically isolate the feed system (cathode potential) from the stand (ground potential). Chilled water for the seals is provided by a closed loop system, discussed in the following section, and is brought to the thrust stand via

copper flexures, as described in Section II B.

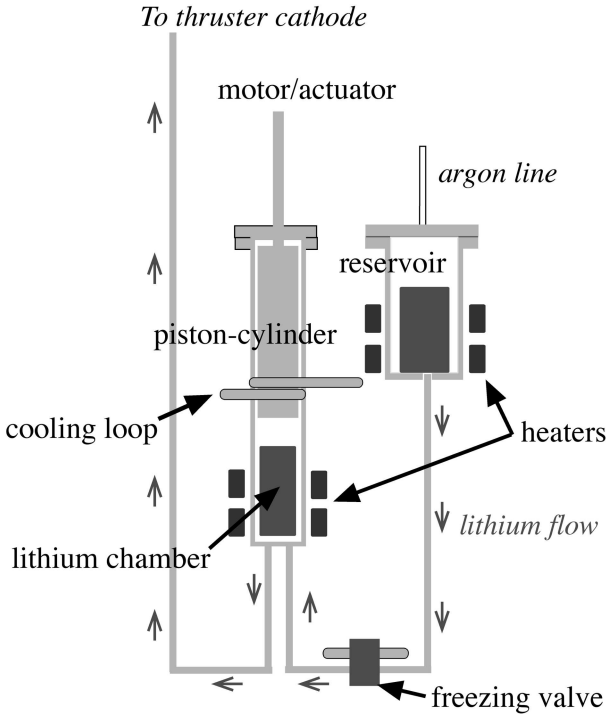

FIG. 4: A schematic of the liquid-lithium feed system. The arrows indicate the path of lithium flow.

C. Facilities

Experiments are conducted in a 1.5 m diameter by 3.6 m steel vacuum chamber. The ultimate pressure is 4×10^{-5} Torr, obtained with a 1.22 m CVC diffusion pump backed by a RUVAC SU2000 roots blower and a 150 CFM Stokes Microvac Pump. Lithium is a condensible propellant that does not raise the pressure during an experiment and thus the effect of pressure on thrust measurement is not a concern. In order to simplify the post-experiment clean-up, the inside of the chamber is covered with aluminum foil, held to the walls by hundreds of small magnets, to capture the lithium as it condenses on the walls. A set of aluminum baffles is mounted approximately 2.7 m from the end of the chamber to block direct flow of lithium into the diffusion pump.

Three separate high-current, DC power supplies are required to operate the MAI LiLFA, plus smaller supplies to heat the feed system. A current-controlled Miller welding power supply provides the thruster with up to 40 kW. The cathode heater is supplied with 1.3 kW at 150 A by an Electronic Measurements, Inc. EMHP power supply. The applied magnetic field solenoid can be provided with up to 230 A by a Rapid Electric Co., Inc. power supply to produce a 0.07 T field. The propellant feed system also requires power to melt and maintain liquid lithium. Three separate 600 W Variacs supply power to the components of the feed system: the reservoir, the piston/cylinder, and the pipes/freezing valve.

Thermal control is achieved with a closed-loop chilled water system. Power dissipated by the solenoid and current conductors, plus the thermal radiation must continuously be removed with the water system to prevent overheating. Two components of the feed system, the lithium freezing valve and the cylinder, rely on water cooling to prevent the flow of liquid lithium where and when it is not desired. Most importantly, the temperature of the thrust stand flexures must be maintained at a constant temperature throughout the experiment to allow thrust measurement. The aforementioned uses of the water system lead to a design that includes five separate water circuits that supply water to different components of the experiment at 125 ml/s each. A high-head pressure model Sta-Rite centrifugal pump supplies up to 630 ml/s at 240 kPa. The heat is rejected to the building chilled water system using SWEP North America Inc. models 10046-030 and 10002-026 water-water heat exchangers.

IV. STEADY STATE THRUST MEASUREMENT OVERVIEW

Two types of stand effects must be taken into account in order to obtain accurate thrust data: 1) long-term thermal drifts and 2) forces other than thrust, including lithium feeding and current-induced forces. Long-term thermal drifts occur for the duration of the experiment (approximately 20 minutes). Whenever the solenoid or thruster current is varied the drift rate or direction changes. To characterize the stand response to each change we allow the stand to drift for four minutes before and after any event. The wait time is based on the time required for the drifts to become linear and have a small magnitude, less than 10% of the PSD range over each portion of the experiment. In our facility, the drift direction and rate roughly correspond to the change in the temperature of the water that flows through the flexures. Careful calibration is required to account for other forces affecting the stand displacement. The two primary forces that add to the thrust measured are due to the propellant feeding and current conduction,

$$F = T + F_{\text{current}} + F_{\text{feeding}}, \tag{3}$$

and will be described in sections IV B and IV C.

A. Thermal Effects on Stand Sensitivity

Perhaps the most troublesome stand behavior is its tendency to drift due to changing thermal loads. In a standard pendulum the harmonic response is ensured by the gravitational force acting on the load. However, with the inverted-pendulum this response becomes dependent on the elasticity of the flexures, i.e. the characteristic mass $M_\star$. For low thrust-to-weight ratio devices the inverted design is more sensitive to applied forces than the traditional pendulum. However, it has the disadvantage of also being sensitive to temperature variations in the flexures. As the flexure temperatures change so does the effective spring constant and thus the sensitivity of the stand.

The evolution of the flexure temperature has three main sources:

- Radiation from the feed system, thruster, and plasma. This effect has been minimized by installing radiation shields around the flexures.
- Joule heating of the flexures due to the current conducted along their length. It is estimated that this contribution will be a maximum of $\approx$200 W per flexure which can raise the cooling water temperature only a fraction of a degree.
- Changes in flexure cooling water temperature is the largest contribution to thermal drift. This effect is unavoidable due to the role of the water in removing heat from the feed system, thruster and solenoid.

The development of these temperature induced drifts in time is governed by the thermal inertia of the water system and the thermal power deposited in it. The water system has a large thermal inertia that results in an overall rate of temperature change that is less than 5° C per hour under conditions of maximum change in thermal power deposition. During an experiment, temperature gradients are limited by allowing most components to reach a steady state temperature and thus constant thermal power deposition. The temperature of the water leaving the thrust stand only varies by a fraction of a degree during a thrust measurement.

B. Lithium Feeding Effects

The placement of the lithium feed system on the thrust stand introduces the possibility that thrust measurements will be adversely effected by vibrations induced by the stepper motor, thermal loads due to feed system heating and cooling requirements, and/or the motion of the piston and lithium on the stand. Vibrational effects due to the operation of the feed system motor were determined to be negligible. The effect of thermal loading has been discussed in the previous section, the contribution from the feed system is a small fraction of the total thermal load. Calibrations of the stand have determined that the stand deflection due to the movement of the piston and lithium during a firing are both small and linear while the piston is moving at a constant velocity. Average slopes of less than $0.1 \pm 1\%$ mV/s are expected at typical lithium feeding rates (10-30 mg/s). This is an order of magnitude smaller than typical drifts due to thermal effects observed during calibrations. Since thrust measurements are taken during periods of constant lithium feeding and the effect is small compared with thermal effects, no further consideration is given to feeding effects.

C. Current-Induced Forces

As current is brought to the thruster and its associated subsystems, the interaction of these current carrying elements produce forces which cannot be easily discriminated from thrust. It is to be noted that this effect is quite complex because the total force exerted on the thrust stand depends not only on the current to one subsystem but on the interaction of all subsystems. The magnetic fields induced by current to the thruster, the cathode heater, and the solenoid interact with each other and also with the field generated by the solenoid to produce a composite effect. Careful distribution of the current paths among the eight current carrying flexures and the placement of cabling within the facility minimizes the effect of the current induced force by creating symmetrical and small area dipoles. The power leads have been twisted and paired to reduce the magnetic field generated.

V. CALIBRATION

Characterization of the thrust stand sensitivity and determination of the current-induced force are the goals of the calibration. First, the region of linear response to force of the thrust stand is determined. Second, the repeatability of the thrust stand deflection to a known force is measured. Third, the force induced by the interaction of the thruster current with the facility is characterized. To find the linear region of the thrust stand, 534 mN of force is applied to the stand by the calibration weights at various stand tilt angles. Coarse measurement of the deflection angle is accomplished with the Crossbow tilt sensor. The resulting fine deflection is measured with the laser based measurement device. It was found that the linear region encompassed approximately $\pm 1°$ from the vertical position.

The repeatability of the stand response to a given

TABLE I: Calibration Data

Thruster Current (A)	Current On (mV/mN)	Current Off (mV/mN)
500	-3.06 ± 0.26	-2.91 ± 0.59
600	-2.97 ± 0.39	-3.05 ± 0.16

force is demonstrated through an extensive calibration procedure. Sensitivity calibration is combined with the measurement of the current induced force to prove repeatability in situations as near a firing as possible. The thruster is shorted during calibration to simulate a firing. The solenoid, cathode heater and feed system are brought to their steady-state operating temperatures. This takes between one and two hours. The thruster current is then brought to the desired value. All subsequent events occur at four minute intervals. This time was chosen to allow the collection of enough data to reduce the uncertainty in the measurement by accurately characterizing the linear stand drift. The calibration procedure is as follows:

- A force of 267 mN is applied with the calibration weights to measure stand sensitivity.
- The thruster current is turned off to measure the deflection of the stand due to the current-induced force.
- Another 267 mN is applied to determine if the sensitivity of the stand is constant.
- The thruster current is turned back on.
- The 534 mN of force is removed.
- The procedure is repeated at least five times for each operation point.

Analysis of the data begins with a linear fit of the recorded stand deflection. Each four minutes of data are fit using an Igor Pro curve fitting macro. The offset, slope and the uncertainties of each fit are noted for the next step. The time at which the calibration weights were removed or the thruster current was turned off is located within the data by the "jumps" in the position data. The lines fitted to the position data just before and after the event are used to determine the deflection of the stand. The difference between the values of the lines gives the change in position of the stand. The uncertainty of the change in stand location is determined from the uncertainties of the coefficients in the two line fits.

We calibrated the thrust stand for a magnetic field of 0.07 T at 500 and 600 A. Table I contains the results of the sensitivity calibration, the first and third steps of the calibration procedure. The sensitivity of the stand was determined by the calibration to be -3.00 ± 0.32 mV/mN.

The current-induced force data, step two of the calibration procedure, was analyzed in manner analogous to the sensitivity data. Unfortunately, the induced force was not as repeatable as that produced by the calibration weights, resulting in an uncertainty greater than 30%, Fig. 5. It can be seen that the data has a tendency to drift during the calibration and the force is not different between 500 and 600 A. At 500 A the induced force, normalized by thruster current, was 0.32 ± 0.08 mN/A and was 0.29 ± 0.13 mN/A at 600 A. The source of the spread in the data is unknown and further calibrations will be required to better understand the stand response.

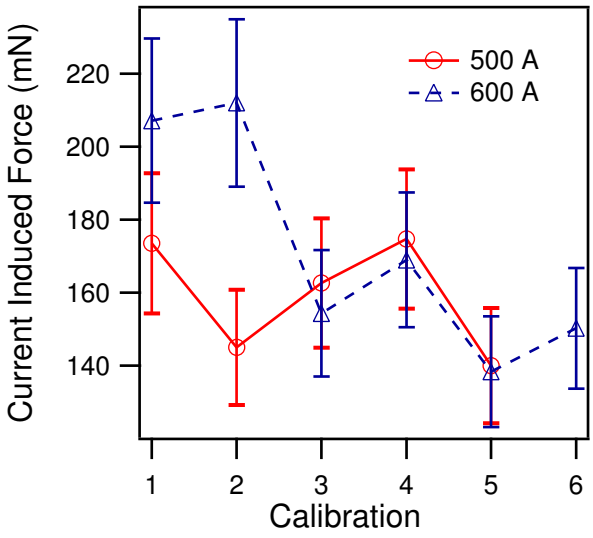

FIG. 5: The current induced force calibration at 500 and 600 A.

VI. SAMPLE THRUST MEASUREMENT

We have measured thrust while operating the MAI LiLFA at 518 A, 9.5 mg/s and 0.07 T magnetic field. The data were not obtained under ideal conditions due to an arc attachment to the stand which caused a premature termination of the experiment. Only a minute of stable current had occurred before the thruster was turned off and a calibration of the stand during the firing was not attempted. Those conditions led to increased error in the measurement because the stand deflection was more difficult to characterize and the drifts did not have a linear slope, Fig. 6. Even with these problems, the effect of thrust could easily be detected by the thrust stand. As noted in the figure, only a small amount of data before and after the thruster was turned off was fit. Using an analysis similar to the calibration, the change in stand deflection as measured by the laser-based measurement device was -297 ± 40 mV. Dividing by the stand sensitivity

and including the uncertainties of both the sensitivity and stand deflection voltage gives a net force of 99 ± 17 mN. The current-induced force acts in the opposite direction of thrust and thus we must calculate this force and add it to the net force to find the thrust. At 518 ± 28 A, the induced force is 166 ± 42 mN. The resulting thrust and thrust efficiency are 265 ± 58 mN and $20 \pm 8\%$, respectively, assuming the uncertainty of the mass flow rate is the same as the uncertainty of the thrust. The large uncertainty is attributed to the vaporization point of lithium not being stabilized within the cathode.

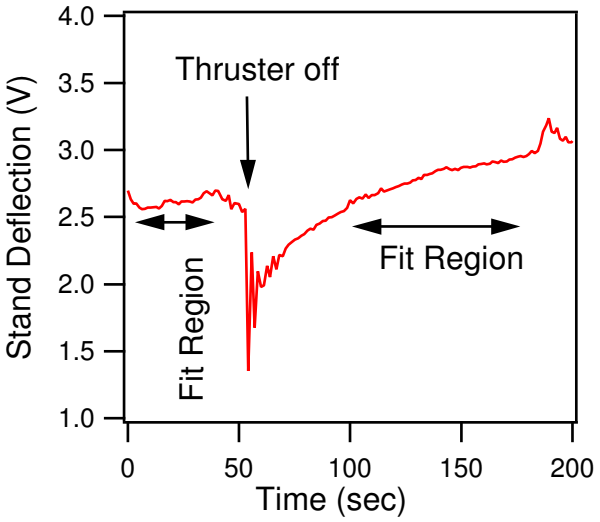

FIG. 6: Raw laser-based measurement system data from the sample thrust measurement.

VII. CONCLUSIONS

The operation of an inverted-pendulum thrust stand for high-power steady-state thrust measurements has been presented. Stand response to a known force has been shown to be linear and repeatable with sensitivities of 3.00 ± 0.32 mV/mN. A procedure for determining forces on the stand due to thruster current and an applied magnetic field has been developed and implemented. Thrust measurement has been demonstrated using the 30 kW applied-field MAI LiLFA. More extensive calibrations of the thrust stand and longer steady-state firings of the thruster are required to reduce the error bars.

VIII. ACKNOWLEDGEMENTS

LiLFA research at EPPDyL is funded by NASA/JPL's Advanced Propulsion Group and the DOE's Plasma Science and Technology program at Princeton University. We would also like to thank Bob Sorenson for his expert technical support of this research, Justin Garretson for his many hours of switch flipping, and Ben Cohen for video support.

[1] R.H. Frisbee and N.J. Hoffman. SP-100 nuclear electric propulsion for Mars cargo missions. In 32^{nd} *Joint Propulsion Conference*, Lake Buena Vista, FL, USA, 1996. AAIAA 96-3173.

[2] J.E. Polk and T.J. Pivirotto. Alkali metal propellants for MPD thrusters. In *AIAA/NASA/OAI Conf. on Advanced SEI Technologies*, Cleveland, Ohio, 1991. AIAA-91-3572.

[3] V.P. Ageyev and V.G. Ostrovsky. High-current stationary plasma accelerator of high power. In 23^{rd} *International Electric Propulsion Conference*, Seattle, WA, USA, 1993. IEPC-93-117.

[4] T. W. Haag. Thrust stand for high power electric propulsion devices. *Rev. Sci. Instrum*, 5:1186–1191, 1991. May.

[5] A. Litvak, J. Lee, and E. Choueiri. Li-LFA thrust stand: Design, fabrication and calibration in open heat pipe lithium lorentz force accelerator: Final technical report for thermacore's phase II SBIR. Technical Report EPPDyL-TR-TC99, EPPDyL-Princeton University, Princeton, NJ, June 1999.

[6] V. Kim, V. Tikhonov, and S. Semenikhin. Fourth quarterly (final) report to NASA-JPL: 100-150 kw lithium thruster research. Technical Report Contract NASW-4851, RIAME, MAI, Moscow, Russia, April 1997.

[7] G. Popov, V. Kim, V. Tikhonov, S. Semenikhin, and M. Tibrina. The fourth quarterly report, contract no 960938 between RIAME MAI and JPL to NASA-JPL. Technical report, RIAME, MAI, Moscow, Russia, December 1998.

[8] Andrea D. Kodys, Gregory Emsellem, Leonard D. Cassady, James E. Polk, and Edgar Y. Choueiri. Lithium mass flow control for high power Lorentz Force Accelerators. In *Space Technology and Applications International Forum*, Albuquerque, New Mexico, USA, 2001. STAIF Paper 195.